Modeling Failure and Fracture in Soft Biological Tissues

Konstantin Y. Volokh

I was neither a student nor a collaborator of Gerhard A. Holzapfel. I learned about him through his very popular constitutive models of soft tissue. I use and appreciate these models. Science still moves forward by small steps that we call new ideas. Not every researcher – even among the able ones – succeeds in proposing something new. Gerhard A. Holzapfel succeeded. Congratulations Gerhard and go ahead!

Kosta

Abstract Soft biological tissues are exposed to moderately large stretches and they are prone to failure and fracture. Failure means the onset of damage and fracture means the damage localization into cracks with their subsequent propagation. There are various approaches to modeling failure and fracture and none of them is superior yet. The description of failure and fracture remains the main challenge in the general field of mechanics of materials for a century. Despite the enormous research effort the progress is mild. In this chapter, our recent work on the topic is briefly reviewed. Our approach is based on two physical assumptions, which avoid the introduction of internal variables. First, we assume that the number and energy of molecular bonds are bounded in a representative volume and, consequently, the macroscopic strain–energy function should also be bounded in the constitutive law. This notion leads to the introduction of energy limiters, which are calibrated in standard tests. Second, we assume that broken bonds are diffused during the fracture process. Such an assumption directly leads to a consideration of the coupled deformation–mass–sink problem. Mathematically, the coupling provides a regularized formulation for modeling crack propagation.

K. Y. Volokh (✉)
Faculty of Civil and Environmental Engineering, Technion – Israel Institute of Technology, 3200003 Haifa, Israel
e-mail: cvolokh@technion.ac.il

G. Sommer et al. (eds.), *Solid (Bio)mechanics: Challenges of the Next Decade*,
Studies in Mechanobiology, Tissue Engineering and Biomaterials 24,
https://doi.org/10.1007/978-3-030-92339-6_17

1 Introduction

Human body comprises soft structures attached to the skeleton. These structures constantly undergo deformation and, sometimes, they can fail and fracture. Tear of meniscus, dissection of arteries, rupture of aneurysms are just a few examples of soft biological tissues that fail and fracture under mechanical deformation. Structural analysis can be helpful for understanding and predicting the load tolerance of parts of human body. It should not be missed that biological tissues are soft and active and their mechanical behavior is strongly nonlinear from both geometric and physical standpoints. Below we review some recent advances in the modeling failure and fracture of soft materials with emphasis on biological tissues. Background information can be found in Volokh (2019a).

2 Failure

Traditional structural analysis is based on the assumption that materials do not fail. Such assumption requires special restrictions on the material models, e.g., polyconvexity, strong ellipticity, Baker-Ericksen inequalities, etc. (Truesdell and Noll 2004). Of course, analytical and numerical methods for the analysis of non-failing materials are relatively simple. However, real materials fail. To describe the failure continuum damage mechanics (CDM) was developed[1] (Simo 1987; Govindjee and Simo 1991; Johnson and Beatty 1993; Miehe 1995; De Souza Neto et al. 1998; Ogden and Roxburgh 1999; Holzapfel 2000; Menzel and Steinmann 2001; Guo and Sluys 2006; De Tommasi et al. 2008; Dal and Kaliske 2009; Li and Holzapfel 2019). The idea of CDM is to decrease material stiffness via an additional damage variable. Such a variable does not have an appealing physical interpretation and, because of that, it is called internal variable. Despite the vague meaning, the use of internal variables pays off in cases where a description of the gradual accumulation of damage is necessary. If the damage is abrupt rather than gradual then there is no need in internal variables and it is only necessary to bound the strain-energy function (Volokh 2013). Such approach of bounding the strain energy with a limiter and its implications are considered in the present section.

2.1 Energy Limiter

Structural analysis means solution of the initial boundary-value problem (IBVP), which includes the linear momentum balance: $\rho\ddot{\mathbf{y}} = \mathrm{Div}\mathbf{P}$; the angular momentum balance: $\mathbf{P}\mathbf{F}^{\mathrm{T}} = \mathbf{F}\mathbf{P}^{\mathrm{T}}$; the constitutive law: $\mathbf{P} = \partial\psi/\partial\mathbf{F}$; and kinematics: $\mathbf{F} = \partial\mathbf{y}/\partial\mathbf{x}$. Here $\mathbf{x} \in \Omega_0$ and $\mathbf{y}(\mathbf{x}) \in \Omega$ denote initial and current positions of a material point

[1] We refer to the works on CDM in which finite strains were considered.

accordingly; ρ is the referential mass density; $\ddot{\mathbf{y}}$ is the acceleration; $\mathbf{P}$ is the first Piola-Kirchhoff stress tensor; and ψ is the strain-energy function. Traction boundary conditions on $\partial\Omega_0$ are given: $\mathbf{Pn} = \bar{\mathbf{t}}$, where $\bar{\mathbf{t}}$ is a prescribed traction and $\mathbf{n}$ is a unit outward normal to $\partial\Omega_0$; or, alternatively, placements are given on $\partial\Omega_0$: $\mathbf{y} = \bar{\mathbf{y}}$. In addition, initial conditions in Ω_0 complete formulation of IBVP: $\mathbf{y}(t = 0) = \mathbf{y}_0$ and $\dot{\mathbf{y}}(t = 0) = \mathbf{v}_0$.

The choice of the strain-energy function ψ is an art. However, a restriction should be imposed on ψ if we wish to include failure in the material description. Indeed, the number of molecules in the body or any part of it is bounded and, consequently, the energy that molecular bonds can accumulate is bounded. Thus, the strain-energy function must be bounded or limited. Various ways to limit the strain energy can be proposed. We use the upper incomplete gamma function (Volokh 2007, 2010), $\Gamma[s, x] = \int_x^\infty t^{s-1}e^{-t}\mathrm{d}t$, in order to bound the strain-energy function, i.e.

$$\psi(\mathbf{F}) = \phi m^{-1}\Gamma[m^{-1}, W(\mathbf{1})^m\phi^{-m}] - \phi m^{-1}\Gamma[m^{-1}, W(\mathbf{F})^m\phi^{-m}]. \tag{1}$$

Here the first term on the right-hand side corresponds to the failure energy and the second term corresponds to the elastic energy. Also, $W(\mathbf{F})$ is the strain-energy function without failure; ϕ is the energy limiter—average bond energy (Volokh 2007); $\mathbf{1}$ is the identity tensor; and m is a material parameter.

Deformation increase beyond a critical threshold leads to the decrease of the elastic energy, which numerically vanishes and the strain energy approaches the failure energy. To make the process irreversible a modification of (1) is necessary (Volokh 2014); however, the irreversibility is important when damage localization is considered and we postpone its consideration to the section on fracture.

The strain-energy function (1) yields the constitutive law

$$\mathbf{P} = \partial\psi/\partial\mathbf{F} = \exp[-W^m\phi^{-m}]\partial W/\partial\mathbf{F}, \tag{2}$$

which does not include any gamma function and only the exponential factor makes difference between the present formulation and traditional hyperelasticity for the intact material behavior.

Examples of the stress-stretch curves for two aneurysm tissues are shown in Fig. 1, where the Cauchy stress tensor $\boldsymbol{\sigma} = J^{-1}\mathbf{P}\mathbf{F}^{\mathrm{T}}$ is used with $J = \det\mathbf{F}$. The intact strain energy is chosen as follows: $W = c_1(\mathbf{F} : \mathbf{F} - 3) + c_2(\mathbf{F} : \mathbf{F} - 3)^2$. Material is incompressible: $J = 1$. Constants for aneurysm tissues 1 and 2 are fitted to the experimental data from Volokh and Vorp (2008) and Raghavan and Vorp (2000) accordingly, see Table 1.

The reader should note that the limit points and downhill branches on the stress-stretch curves are a direct consequence of the limited strain energy. Without limiting the strain energy we would get stresses going to infinity with the increasing stretch, which is evidently nonphysical. We should also note that damage localizes after the limit point, while it is implied that the state of the deformation state is uniform in uniaxial tests. To overcome this interpretation difficulty the reader might imagine

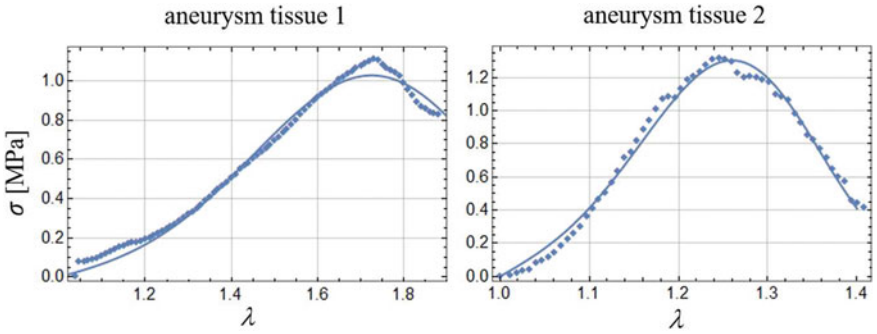

Fig. 1 Cauchy stress versus stretch in uniaxial tension for two aneurysm tissues: solid curves denote modeling and diamonds denote experimental data. Reprinted from Volokh and Vorp (2008) and Volokh (2015), with permission from Elsevier and Springer accordingly

Table 1 Material constants

	c_1 [MPa]	c_2 [MPa]	ϕ [MPa]	m [–]
Aneurysm tissue 1	0.103	0.18	0.402	1
Aneurysm tissue 2	0.52	3.82	0.255	1

that the experiment is done inside a black box. The only measurable quantities are stresses and stretches of a specimen at the entry and exit of the box. Thus, stretches can increase with the decreasing stresses after damage and rupture. Specific localization of damage is of minor importance in the case of repeatability of the experimental results.

In the following subsections we consider various applications of the proposed formulation concerned with the prediction of failure.

2.2 Cavitation

Remodeling of soft tissues can be accompanied by morphological changes that can lead to appearance of micro-voids. Cavitation is defined as a sudden irreversible expansion of micro-voids into visible macroscopic voids. Such a failure mode is often a predecessor of cracks in soft materials.

Mathematically, the void expansion in isotropic material can be described by the following integral formula

$$p(\lambda_a) = \int_1^{\lambda_a} \frac{1}{\lambda^3 - 1} \frac{\mathrm{d}\hat{\psi}}{\mathrm{d}\lambda} \mathrm{d}\lambda, \tag{3}$$

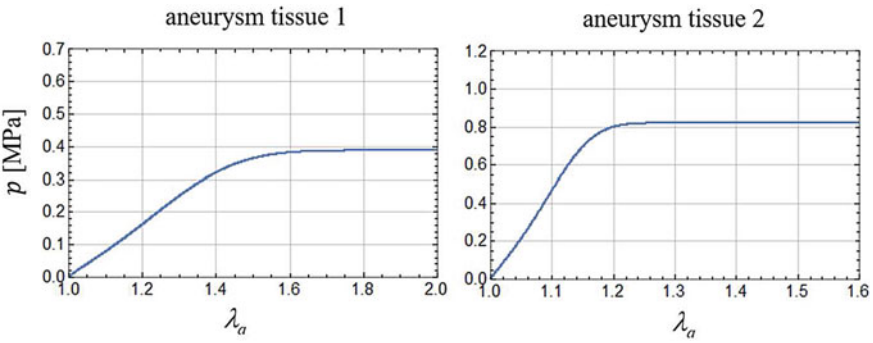

Fig. 2 Hydrostatic tension versus hoop stretch for void growth. Reprinted from Volokh (2015), with permission from Springer

where p is the remote hydrostatic tension; λ is the hoop stretch; $\lambda_a = a/A$ with A and a denoting the initial and current radius of the void accordingly; and the strain energy is expressed in terms of the principal stretches $\lambda_1, \lambda_2, \lambda_3$ for incompressible material: $\hat{\psi}(\lambda) = \psi(\lambda_1, \lambda_2, \lambda_3) = \psi(\lambda^{-2}, \lambda, \lambda)$.

Substituting two tissue models described above in (3), it is possible to draw curves shown in Fig. 2 (Volokh 2015).

The curves reach the tension limit with the increasing hoop stretch. At this limit the void expansion becomes unstable because it does not require a pressure increase. This is the critical cavitation tension. It cannot be overstated that the critical tension can only be reached for material models incorporating a failure description (Volokh 2011; Lev and Volokh 2016). Remarkably, unstable growth of cavities can start under critical stresses that are considerably less than the aneurysm strength. Also, we should note that the state of the hydrostatic tension triggering the unstable cavity expansion can occur in the vicinity of rigid inclusions. Thus, tissue calcification can be a qualitative indicator of a possible onset of rupture.

2.3 Calcification

Calcification is an abnormal accumulation of calcium salts in soft tissue causing it to harden. We modeled tension of aneurysm material including stiff calcified particles (Volokh and Aboudi 2016). Particularly, we analyzed the effect of the varying amount of calcification (10, 40, and 70%), i.e. the relative volume of the hard inclusion within the periodic elementary cell, on the tissue stiffness and strength, see Fig. 3.

We found that the increase of the relative volume of calcium particles unconditionally led to the stiffening of the tissue. However, the strength did not increase in the most considered cases—it could significantly decrease. The drop of the strength varied from 10 to 40% and more. This finding emphasizes the difference between

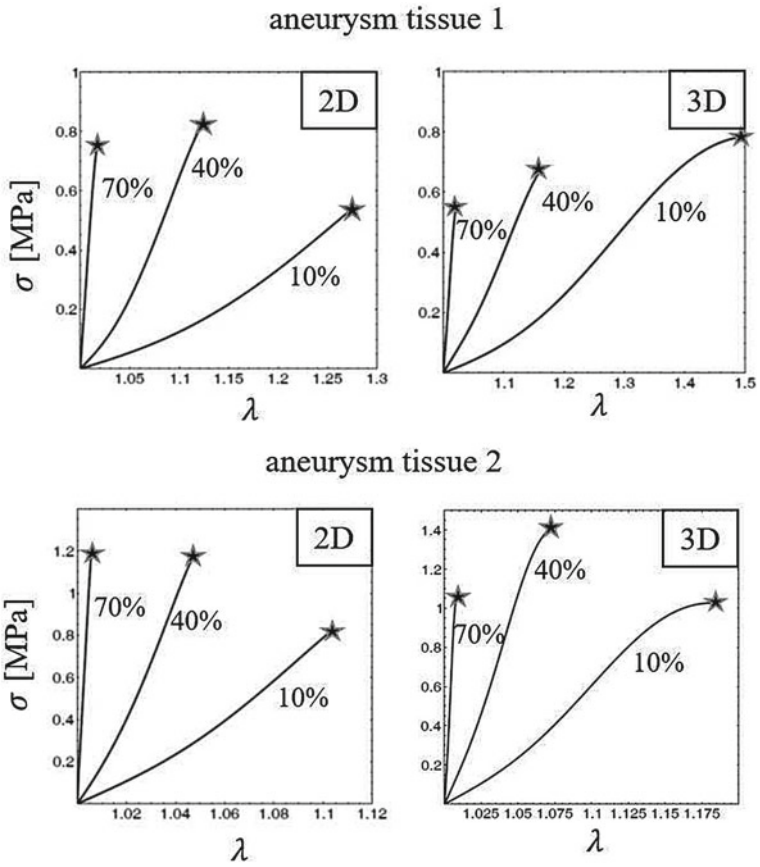

Fig. 3 Cauchy stress versus stretch in uniaxial tension for aneurysm tissues with varying calcification. Stars denote points beyond which static solution does not exist—strength. Reprinted from Volokh and Aboudi (2016), with permission from Springer

the concepts of stiffness and strength. The strength of a composite is significantly influenced by the locally inhomogeneous deformation. Hard particles can be stress concentrators amplifying the likelihood of the local material failure.

Besides, the hard particles restrain deformation in their vicinity creating a state of hydrostatic tension which, in its turn, can trigger cavitation with the subsequent fracturing. Figure 4 shows the maps of the triaxiality ratio defined by formula $\mathrm{tr}\boldsymbol{\sigma}\,(27\mathrm{dev}\boldsymbol{\sigma} : \mathrm{dev}\boldsymbol{\sigma}/2)^{-1/2}$, where 'tr' and 'dev' denote the trace and the deviatoric part of a second-order tensor, respectively. High triaxiality ratios appear at the poles of hard inclusions. These are locations where damage starts.

It is worth emphasizing that smaller calcified particles might be more dangerous from the standpoint of strength. Consequently, the tissues at initial stages of calcification might be more prone to rupture!

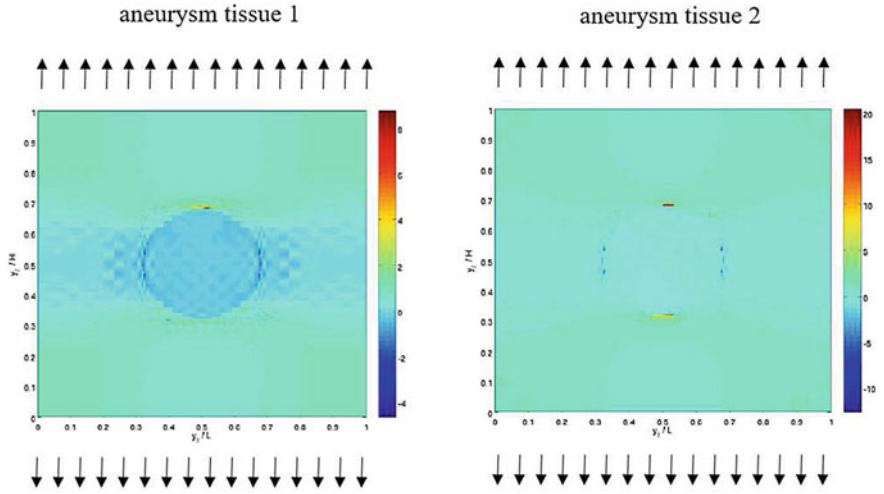

Fig. 4 Triaxiality ratio $\mathrm{tr}\boldsymbol{\sigma}\,(27\mathrm{dev}\boldsymbol{\sigma} : \mathrm{dev}\boldsymbol{\sigma}/2)^{-1/2}$ distribution for 10% calcification for aneurysm tissues at the failure load. Reprinted from Volokh and Aboudi (2016), with permission from Springer

The obtained results have limitations because an ideally periodic distribution of calcified particles was assumed in computations while in reality the distribution is random. Thus, additional research in stochastic mechanics of failure analysis is required.

2.4 Crack Direction

The idea of predicting the onset of the damage and the the direction of its localization—crack—can be qualitatively described as follows. Intact material can propagate superposed plane waves defined by vector $\mathbf{r}g(\mathbf{s}\cdot\mathbf{y}-vt)$, where $\mathbf{r}$ and $\mathbf{s}$ are the unit vectors in the directions of the wave polarization and wave propagation, respectively, and v is the wave speed. However, cracks become barriers on the way of the wave propagation. Within cracks a material is damaged and, consequently, a superposed wave cannot run in the direction perpendicular to the damage localization. The latter notion prompts the idea to find the crack direction: it is necessary to find a direction in which the superposed wave has zero speed (Volokh 2017a; Mythravaruni and Volokh 2018, 2019, 2020; Volokh 2019b).

Mathematically, the condition of the zero wave speed can be written as

$$\rho v^2 = s_j s_l r_i r_k F_{js} F_{lr} \frac{\partial^2 \psi}{\partial F_{is}\partial F_{kr}} = 0, \tag{4}$$

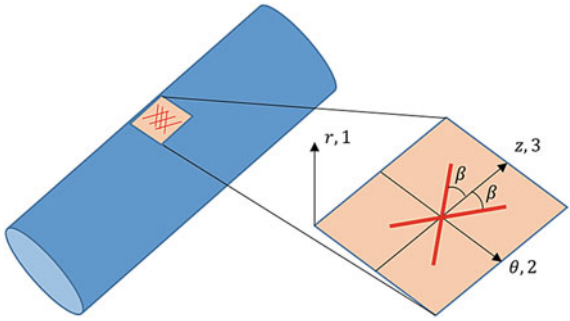

Fig. 5 Radial (1 or r), circumferential (2 or θ), and longitudinal (3 or z) directions in artery. Reprinted from Raghavan and Vorp (2000), with permission from Springer

Table 2 Material constants

c [kPa]	k_1 [kPa]	k_2 [–]	ϕ [kPa]	m [–]	β [°]
75	1500	0.03	95	1.2	45.8

where, accounting for (1),

$$\frac{\partial^2\psi}{\partial F_{is}\partial F_{kr}} = \left(\frac{\partial^2 W}{\partial F_{is}\partial F_{kr}} - mW^{m-1}\phi^{-m}\frac{\partial W}{\partial F_{kr}}\frac{\partial W}{\partial F_{is}}\right)\exp[-W^m\phi^{-m}]. \tag{5}$$

We illustrate the use of this condition via example of arterial tissue, which is anisotropic due to two families of oriented bundles of collagen fibers, see Fig. 5.

Following Volokh (2019b), we consider the strain energy in the form

$$\begin{aligned}\psi = {} & c(\mathbf{F}:\mathbf{F}-3)/2 + 2\phi m^{-1}\Gamma[m^{-1},0] - \phi m^{-1}\Gamma[m^{-1},W_4^m\phi^{-m}] \\ & -\phi m^{-1}\Gamma[m^{-1},W_6^m\phi^{-m}],\end{aligned} \tag{6}$$

where

$$W_{4,6} = k_1\{\exp[k_2\left\langle\left|\mathbf{F}\mathbf{m}_{4,6}\right|^2-1\right\rangle]-1\}/(2k_2), \quad [\mathbf{m}_{4,6}] = [0,\pm\sin\beta,\cos\beta]^{\mathrm{T}}. \tag{7}$$

Here, triangle Macaulay brackets are used to account for the fiber response in tension only: $\langle x\rangle = x$ for positive x and $\langle x\rangle = 0$ otherwise. Unit vectors $\mathbf{m}_4$ and $\mathbf{m}_6$ denote two families of collagen fibers. Based on the experimental data kindly provided by the Institute of Biomechanics at Graz University of Technology, it was possible to calibrate the model (see Fig. 6), and the material constants are given in Table 2 (Volokh 2019b).

Since it is assumed that the material is incompressible, we consider the propagation of the superimposed transverse or shear waves in the plane that is tangent to the artery, see Fig. 5. These waves are defined by the following mutually orthogonal

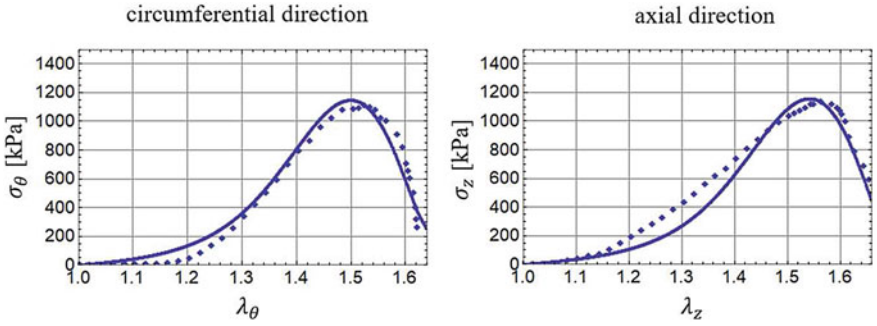

Fig. 6 Stress-stretch curves for arterial tissue: solid curves for the theory and diamonds for the experimental data. Reprinted from Volokh (2019b), with permission from Springer

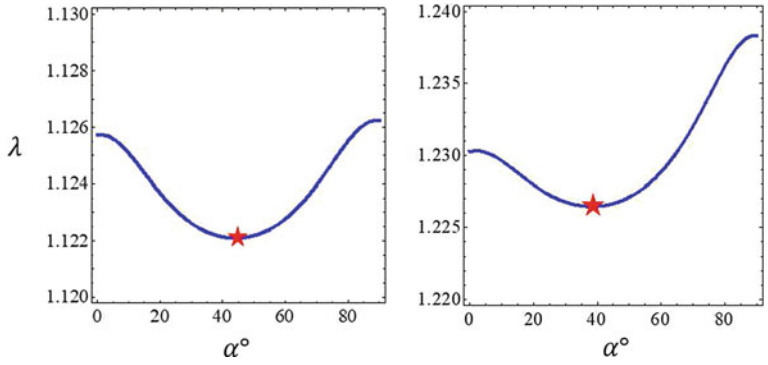

Fig. 7 Equibiaxial tension (left) and pure shear (right): $\rho v^2(\lambda, \alpha) = 0$ (stars show minima). Reprinted from Volokh (2019b), with permission from Springer

unit vectors: $[\mathbf{s}] = [0, \sin\alpha, \cos\alpha]^{\mathrm{T}}$ and $[\mathbf{r}] = [0, \cos\alpha, -\sin\alpha]^{\mathrm{T}}$. We also limit our considerations by equibiaxial and pure shear deformations. In these cases only one stretch λ describes the deformation. Thus, we have only two independent variables λ and α and (4) takes on the form: $\rho v^2(\lambda, \alpha) = 0$. Curves which are given by this equation are presented in Fig. 7. Starred points in Fig. 7 give the minimum stretches λ at which materials fail and damage starts localizing. Angles α correspond to the minima and provide directions perpendicular to the damage localization in the current configuration. The latter notion makes it possible to predict the direction of the future crack. In the considered examples,the directions of the cracks are aligned with the direction of the fibers. This finding agrees with the reported experiments by Luo et al. (2016) where the authors concluded that 'the direction of the rupture … is aligned with the direction of maximum stiffness', which is the direction of fibers.

In the considered example, we used the assumption of material incompressibility. Such assumption can be effective for the creation of analytical solutions, as Ronald Rivlin has demonstrated at length in his work. However, from our perspective there is

an unfavorable side to the incompressibility assumption: it suppresses the consideration of longitudinal or pressure waves. Such waves might give important predictions concerning the onset of cracks and they cannot be ignored (Mythravaruni and Volokh 2019). The incompressibility constraint can turn into a Trojan Horse in the analysis!

In the light of remarks concerning the incompressibility enforcement we refer to (Mythravaruni and Volokh 2020) where the constraint was relaxed and both superimposed transverse and longitudinal waves were considered as well as fiber the dispersion was introduced in the constitutive setting. The vanishing pressure wave speed predicted cracks in the direction perpendicular to the tension in the uniaxial tension and pure shear. The vanishing shear wave speed predicted cracks in the direction inclined to tension in the uniaxial tension and pure shear. Equibiaxial stretching can lead to the appearance of cracks in any direction despite the anisotropy of material. The inclined cracks oriented along the bundles of collagen fibers were experimentally found and reported in Sugita and Matsumoto (2017).

3 Fracture

Hyperelastic models with energy limiters described above cannot be directly used for the modeling of damage localization and propagation. The reason is that the numerical solution of the IBVP becomes mesh-dependent. The thickness of the damaged area or crack is equal to the size of a cell in the spatial discretization mesh. Reducing the cell size one reduces the thickness of the damage localization area, which, in its turn, reduces the energy dissipated during the fracture process. Ultimately, the dissipated energy vanishes with mesh refinement. Thus, fracture can theoretically occur without any dissipated energy. The latter possibility is physically meaningless, of course. The described pathology is inherent in any continuum damage theory and not only the theory described above.

A way to suppress the pathological mesh sensitivity is to introduce strong discontinuity defined by a cohesive surface with a traction-separation constitutive law. In this way, we immediately have two new surfaces representing crack. Unfortunately, the surface nucleation, orientation, branching and arrest require extra criteria, which are not a part of constitutive description. Even worse, cohesive surface formulations presume a simultaneous use of different constitutive models: one for the surface traction-separation and another for the intact bulk material. Correspondence between these two constitutive theories is not readily available.

A more attractive way to suppress the pathological mesh sensitivity would be a regularization of continuum damage theories preventing from zero energy fractures. For the latter purpose, nonlocal continuum formulations were invented where a characteristic length was incorporated to limit the size of the spatial damage localization (Pijaudier-Cabot and Bazant 1987; Lasry and Belytschko 1988; Peerlings et al. 1996; Francfort and Marigo 1998; Silling 2000). In some of these formulations, e.g., the internal damage variable is described by an additional differential equation of the reaction-diffusion type. In this equation, the highest spatial derivatives of the

damage variable are scaled by a characteristic length providing solutions of the boundary layer type. Such layer is interpreted as a diffused crack of finite thickness. A special choice of the regularizing equation, called phase-field approach, gained popularity in recent years (Hofacker and Miehe 2012; Borden et al. 2012; Denli et al. 2020). It is claimed that the phase-field formulation yields convergence of the diffused crack to the surface of discontinuity under the decrease of the characteristic length, which is interpreted as a varying numerical parameter. However, an analysis of the simple uniaxial tension shows that, in the phase-filed formulation, the characteristic length is a fixed physical parameter linked to material strength.[2]

The regularization strategy rooted in nonlocal continua formulations is attractive because it is coherent mathematically. Regrettably, the generalized nonlocal continua theories are based on the physical assumption of long-range particle interactions, while the actual particle interactions are short-range involving only the closest neighbors. Therefore, the physical basis for the nonlocal models appears disputable. A more physically based treatment of the pathological mesh sensitivity should probably include multi-physics coupling as we show below.

3.1 Material Sink

We can see crack surfaces and we rightfully conclude that these surfaces are a result of material separation. However, we usually take another logical step and assume that the separation surfaces is a result of the debonding of two adjacent atomic or molecular layers, see Fig. 8, left. The latter assumption is the simplest and, therefore, speaks to intuition. However, this assumption contradicts routine observations that cracks are visible to the naked eye, see Fig. 8, center. Indeed, if the separation was between two adjacent atomic layers, then we would not see closed cracks because our eye can only distinguish objects on the micrometer scale and not angstroms. Thus, the crack surfaces are not created by two adjacent atomic layers—they are created by a massive bond breakage spread over a region with a characteristic length l, Fig. 8, right.

The process of the bond breakage is diffusive rather than confined to two atomic planes! Some atoms fly out of the bulk material. Generally, we cannot see them because of their very small amount, as compared to the bulk. Sometimes, we can see them—remember the dust of fracturing brittle concrete. The characteristic length of the damaged region is large enough for observing small disintegrated pieces of concrete.

The notion of material sink within the characteristic small region gives rise to a mathematical formulation in which momenta and mass balance are coupled (Volokh 2017b). We add the mass balance in Ω_0 to the governing equations

[2] For example, the authors rightfully note in Borden et al. (2012) that 'although the length-scale parameter associated with the phase-field approximation is introduced as a numerical parameter it is, in fact, a material parameter that influences the critical stress at which crack nucleation occurs.'

Fig. 8 Left: idealized crack with zero thickness; center: visible closed crack in unloaded tire; right: realistic bulk crack with finite thickness l

$$\mathrm{Div}\mathbf{s} + \xi = 0, \tag{8}$$

where $\mathbf{s}$ and ξ are the referential mass flux and source (sink) accordingly.

The mass balance on the boundary $\partial\Omega_0$ provides the natural boundary condition

$$\mathbf{s} \cdot \mathbf{n} = 0. \tag{9}$$

We note that the mass balance is used in the reduced form $\mathrm{Div}\mathbf{s} + \xi = 0$ instead of $\dot{\rho} = \mathrm{Div}\mathbf{s} + \xi$ because we are only interested in pre- and post- cracked states, while the transition process of the bond rupture is so fast that it can be neglected. Such simplification is analogous to consideration of the buckling process in thin-walled structures, in which pre- and post–buckled states are analyzed by using a time-independent approach and the fast dynamic transition to the buckled state is ignored.

Skipping details given in Volokh (2017b), we define constitutive laws for the stress

$$\mathbf{P} = (\rho/\rho_0)\partial W/\partial \mathbf{F}, \tag{10}$$

the mass sink

$$\xi = \beta\rho_0 H(\gamma)\exp[-W^m\phi^{-m}] - \beta\rho, \tag{11}$$

and the mass flux

$$\mathbf{s} = \kappa H(\gamma)\exp[-W^m\phi^{-m}]J(\mathbf{F}^{\mathrm{T}}\mathbf{F})^{-1}\partial\rho/\partial\mathbf{x}, \tag{12}$$

where $\rho_0 = \rho(t=0)$ is the initial density; $\beta > 0$ and $\kappa > 0$ are material constants; $H(\gamma)$ is a unit step function, i.e. $H(\gamma) = 0$ if γ is negative and $H(\gamma) = 1$ otherwise; the switch parameter $\gamma \in (-\infty, 0]$ is necessary to prevent from the material healing and it is defined by the evolution equation $\dot{\gamma} = -H(\epsilon - \rho/\rho_0)$, $\gamma(t=0) = 0$ where $0 < \epsilon \ll 1$ is a dimensionless precision constant.

It is worth noting that the elasticity with energy limiters emerges as a particular case of the present formulation when there is no damage localization via diffusion of broken bonds. Indeed, if mass flux and sink are not active, $\mathbf{s} = \mathbf{0}$ and

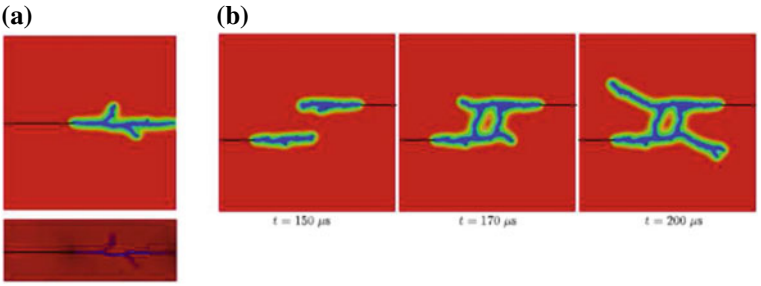

Fig. 9 (a) Propagation of Mode 1 crack in aneurysm tissue 2 in current (top) and referential (bottom) configurations; (b) crack bridging and kinking. Reprinted from Faye et al. (2019), with permission from Springer

$\xi = 0$, then we calculate from (11): $\rho/\rho_0 = H(\gamma)\exp[-W^m\phi^{-m}]$. Since the irreversibility is not important in this case, we set $H(\gamma) \equiv 1$ and further simplify: $\rho/\rho_0 = \exp[-W^m\phi^{-m}]$. Substitution of the latter formula in (10) yields (2).

3.2 *Dynamic Fracture*

The onset and localization of damage are usually related to the loss of the static stability. Beyond the static instability point the process becomes dynamic. The latter is the reason why most cracks propagate dynamically unless they are highly restrained. We implemented the material sink formulation presented above in analysis of dynamic crack propagation in aneurysm tissue 2 (Faye et al. 2019).

We note that the substitution of (11) and (12) in (8) yields the following second-order partial differential equation with respect to the referential mass density ρ, i.e.

$$l^2\mathrm{Div}\{H(\gamma)\exp[-W^m\phi^{-m}]J(\mathbf{F}^{\mathrm{T}}\mathbf{F})^{-1}\partial\rho/\partial\mathbf{x}\} + \rho_0 H(\gamma)\exp[-W^m\phi^{-m}] - \rho = 0. \tag{13}$$

Remarkably, we do not need to know material constants κ and β separately. We only need to know their ratio, which defines the characteristic length: $l^2 = \kappa/\beta$. The length is a small multiplier for the highest (second) spatial derivative of the mass density and, consequently, it causes solution of the boundary layer type. This layer regularizes the crack thickness and suppresses the pathological mesh sensitivity.

Results of modeling propagation of a single crack and bridging of two cracks are shown in Fig. 9. These simulations led to the following interesting conclusions.

First, the inertia forces play a crucial role at the tip of the propagating crack. If inertia is not canceled together with the material stiffness, then cracks tend to nonphysically widen with the increasing speed of their propagation. Most existing models of cracks completely ignore this fact and they do not cancel inertia when they cancel stiffness. Only very recently, phase-field modelers started recognizing

the importance of canceling inertia (Chen et al. 2017; Agrawal and Dayal 2017). Needless to say, the simultaneous cancelation of stiffness and inertia are a direct consequence of the material sink formulation presented in this chapter.

Second, the proposed material sink formulation enables the suppression the strong or classical pathological mesh sensitivity associated with the zero energy fracture. The latter is due to the fact that the augmented initial boundary-volume problem enforces the characteristic length and solutions of the boundary layer type. Such layer, associated with the crack thickness, does not vanish under mesh refinement.

Third, we observed a weak mesh sensitivity, which we defined as the effect of the mesh shape and size on the specific crack pattern. We found that various meshes caused slightly different crack patterns for the same amount of dissipated energy. The weak mesh sensitivity remained even after a significant mesh refinement, which showed that the regularized formulations were not a universal recipe as many would expect. The weak mesh sensitivity is similar to the effect of structural inhomogeneities in real materials, which affect the crack path depending on the specific sample under consideration. Though all samples are made of the same material they have various microstructural patterns and, consequently, slightly different propagating cracks.

4 Conclusions

We showed that physically reasonable assumptions of the bounded bond energy and diffused bond breakage were enough for macroscopic analysis of the onset of material damage and its localization into cracks with their subsequent propagation.

The energy of molecular bonds is always bounded because the number of molecules is finite. This automatically implies that the macroscopic strain-energy function must be limited. If the strain energy is limited then the stress cannot approach infinity with increasing strain, the stress must be limited and drop to zero. The limiting stress indicates the onset of material instability or failure, which can be interpreted as inability of material to bear further load. The phenomena of cavitation, strength under calcification, and even direction of possible cracks in soft tissues can be understood based on the approach of elasticity with energy limiters.

Failure is the onset of the damage process. Fracture is the development of damage, its localization, and propagation. Microscopically, the process of fracture means bond breakage. The breakage can hardly be confined to two adjacent molecular layers. Broken bonds are diffused and, because of that, material can be lost locally. Material sink during fracture prompts a macroscopic continuum mechanics formulation based on coupled momenta and mass balance. Such formulation naturally provides regularization of crack simulations suppressing the pathological mesh sensitivity.

Assumptions and methods considered above allow avoiding the use of internal variables, and hence make the theory appealing from the physics standpoint.

Acknowledgements This research was supported by the ISRAEL SCIENCE FOUNDATION (grant No. 394/20).

References

Agrawal, V., Dayal, K.: Dependence of equilibrium Griffith surface energy on crack speed in phase-field models for fracture coupled to elastodynamics. Int. J. Fract. **207**, 243–249 (2017)

Borden, M.J., Verhoosel, C.V., Scott, M.A., Hughes, T.J.R., Landis, C.M.: A phase-field description of dynamic brittle fracture. Comp. Methods Appl. Mech. Eng. **217–220**, 77–95 (2012)

Chen, C.H., Bouchbinder, E., Karma, A.: Instability in dynamic fracture and the failure of the classical theory of cracks. Nat. Phys. **13**, 1186 (2017)

Dal, H., Kaliske, M.: A micro-continuum-mechanical material model for failure of rubberlike materials: application to ageing-induced fracturing. J. Mech. Phys. Solids **57**, 1340–1356 (2009)

De Souza Neto, E.A., Peric, D., Owen, D.R.J.: Continuum modeling and numerical simulation of material damage at finite strains. Arch. Comp. Methods Eng. **5**, 311–384 (1998)

De Tommasi, D., Puglisi, G., Saccomandi, G.: Localized vs diffuse damage in amorphous materials. Phys. Rev. Lett. **100**, 085502 (2008)

Denli, F.A., Gültekin, O., Holzapfel, G.A., Dal, H.: A phase-field model for fracture of unidirectional fiber-reinforced polymer matrix composites. Comput. Mech. **65**, 1149–1166 (2020)

Faye, A., Lev, Y., Volokh, K.Y.: The effect of local inertia around the crack tip in dynamic fracture of soft materials. Mech. Soft Mater. **1**, 4 (2019)

Francfort, G.A., Marigo, J.J.: Revisiting brittle fracture as an energy minimization problem. J. Mech. Phys. Solids **46**, 1319–1342 (1998)

Govindjee, S., Simo, J.C.: A micro-mechanically based continuum damage model of carbon black-filled rubbers incorporating the Mullins effect. J. Mech. Phys. Solids **39**, 87–112 (1991)

Guo, Z., Sluys, L.: Computational modeling of the stress-softening phenomenon of rubber like materilas under cyclic loading. Eur. J. Mech. A/Solids **25**, 877–896 (2006)

Hofacker, M., Miehe, C.: Continuum phase field modeling of dynamic fracture: variational principles and staggered FE implementation. Int. J. Fract. **178**, 113–129 (2012)

Holzapfel, G.A.: Nonlinear Solid Mechanics. A Continuum Approach for Engineering, Wiley, Chichester (2000)

Johnson, M.A., Beatty, M.F.: A constitutive equation for the Mullins effect in stress controlled in uniaxial extension experiments. Cont. Mech. Therm. **5**, 301–318 (1993)

Lasry, D., Belytschko, T.: Localization limiters in transient problems. Int. J. Solids Struct. **24**, 581–597 (1988)

Lev, Y., Volokh, K.Y.: On cavitation in rubberlike materials. J. Appl. Mech. **83**, 044501 (2016)

Li, K., Holzapfel, G.A.: Multiscale modeling of fiber recruitment and damage with a discrete fiber dispersion method. J. Mech. Phys. Solids **126**, 226–244 (2019)

Luo, Y., Duprey, A., Avril, S., Lu, J.: Characteristics of thoracic aortic aneurysm rupture in vitro. Acta. Biomater. **42**, 286–295 (2016)

Menzel, A., Steinmann, P.: A theoretical and computational framework for anisotropic continuum damage mechanics at large strains. Int. J. Solids Struct. **38**, 9505–9523 (2001)

Miehe, C.: Discontinuous and continuous damage evolution in Ogden-type large-strain elastic materials. Eur. J. Mech. A/Solids **14**, 697–720 (1995)

Mythravaruni, P., Volokh, K.Y.: Failure of rubber bearings under combined shear and compression. J. Appl. Mech. **85**, 074503 (2018)

Mythravaruni, P., Volokh, K.Y.: On incompressibility constraint and crack direction in soft solids. J. Appl. Mech. **86**, 101004 (2019)

Mythravaruni, P., Volokh, K.Y.: On the onset of cracks in arteries. Mol. Cell Biomech. **17**, 1–17 (2020)

Ogden, R.W., Roxburgh, D.G.: A pseudo-elastic model for the Mullins effect in filled rubber. Proc. R . Soc. Lond. Ser. A **455**, 2861–2877 (1999)
Peerlings, R.H.J., de Borst, R., Brekelmans, W.A.M., de Vree, J.H.P.: Gradient enhanced damage for quasi-brittle materials. Int. J. Num. Methods Eng. **39**, 3391–3403 (1996)
Pijaudier-Cabot, G., Bažant, Z.P.: Nonlocal damage theory. J. Eng. Mech. **113**, 1512–1533 (1987)
Raghavan, M.L., Vorp, D.A.: Toward a biomechanical tool to evaluate rupture potential of abdominal aortic aneurysm: identification of a finite strain constitutive model and evaluation of its applicability. J. Biomech. **33**, 475–482 (2000)
Silling, S.A.: Reformulation of elasticity theory for discontinuities and long-range forces. J. Mech. Phys. Solids **48**, 175–209 (2000)
Simo, J.C.: On a fully three-dimensional finite strain viscoelastic damage model: formulation and computational aspects. Comput. Methods Appl. Mech. Eng. **60**, 153–173 (1987)
Sugita, S., Matsumoto, T.: Local distribution of collagen fibers determines crack initiation site and its propagation direction during aortic rupture. Biomech. Model. Mechnobiol. **17**, 577–587 (2017)
Truesdell, C., Noll, W.: The Non-Linear Field Theories of Mechanics. Springer, Berlin (2004)
Volokh, K.Y.: Hyperelasticity with softening for modeling materials failure. J. Mech. Phys. Solids **55**, 2237–2264 (2007)
Volokh, K.Y., Vorp, D.A.: A model of growth and rupture of abdominal aortic aneurysm. J. Biomech. **41**, 1015–1021 (2008)
Volokh, K.Y.: On modeling failure of rubberlike materials. Mech. Res. Commun. **37**, 684–689 (2010)
Volokh, K.Y.: Cavitation instability in rubber. Int. J. Appl. Mech. **3**, 29311 (2011)
Volokh, K.Y.: Review of the energy limiters approach to modeling failure of rubber. Rubber Chem. Technol. **86**, 470–487 (2013)
Volokh, K.Y.: On irreversibility and dissipation in hyperelasticity with softening. J. Appl. Mech. **81**, 074501 (2014)
Volokh, K.Y.: Cavitation instability as a trigger of aneurysm rupture. Biomech. Model. Mechanobiol. **14**, 1071–1079 (2015)
Volokh, K.Y., Aboudi, J.: Aneurysm strength can decrease under calcification. J. Mech. Behav. Biomed. Mater. **57**, 164–174 (2016)
Volokh, K.Y.: Loss of ellipticity in elasticity with energy limiters. Eur. J. Mech. A/Solids **63**, 36–42 (2017a)
Volokh, K.Y.: Fracture as a material sink. Mater. Theory **1**, 3 (2017b)
Volokh, K.Y.: Mechanics of Soft Materials. Springer, Singapore (2019a)
Volokh, K.Y.: Constitutive model of human artery adventitia enhanced with a failure description. Mech. Soft Mater. **1**, 8 (2019b)